Numerical Modeling of Experimentally Obtained Lightning Arc Root Damage in Metal Sheets

Yulia Kostogorova-Beller[1], Tianshi Lu*[2]

[1]National Institute for Aviation Research, 1845 Fairmount St, Wichita, KS 67260-0093, USA
[2]Department of Mathematics, Statistics and Physics, Wichita State University, Wichita, Kansas 67260-0033, USA
[1]yulia@niar.wichita.edu; *[2] lu@math.wichita.edu

Abstract

This work investigates the evolution of simulated lightning-induced damage in aluminum cathode sheets based on the experimental evidence and numerical modelling. Quasi-equilibrium thermal plasma discharges characterized by the 50-950 A arc currents transferring up to 770 C of charge were utilized to experimentally investigate damage development at atmospheric pressure in air. Heat-conduction model was developed to computationally study the damage resulting from the lightning root attachment to the metal surface. It was demonstrated that the metal melting in contrast to evaporation was dominant in damage formation. The effective voltage drop in the range of 10.5-13 V for aluminum sheet cathodes was identified and utilized in modelling. The proposed model predicts damage formation in 50-950 A arcs with 200 C charge transfer. The inferred range of voltage drop lies in close proximity to the true cathode falls reported in literature. Both the experiment and the numerical modelling indicate that the damage volume in a thin metal sheet induced by lightning arcs is proportional to the charge transfer. The ratio, a material-dependent constant which is higher for metals with lower melting point, was computed for various metals, including aluminum alloy for which the computed value was in good agreement with the experimental data.

Keywords

Lightning Arc Damage; Airframe Structure; Lightning Protection; Aluminum Cathode Sheet; Heat Conduction; Cathode Voltage Drop; Numerical Modelling

Introduction

A direct lightning attachment to composite airframe structures presents a potential hazard of a catastrophic failure in contrast to aluminum structural components whose high electrical and thermal conductivities provide an inherent protection against lightning for an aircraft in flight. A growing usage of fiber-reinforced polymer-matrix composites in aircraft and aerospace industries has drastically increased demand for the ability to model the destructive effects of lightning; however, prediction of their response is complicated due to the anisotropic and inhomogeneous nature of the composites. The direct lightning interaction mechanisms with aircraft structural components are difficult to define precisely due to the lack of data and study in this field, and although a lot of modelling has been previously implemented, a congruent work demonstrating the extent of lightning damage successfully supported by the computer-simulated outcome in either metallic or composite specimens only begins to emerge in the lightning scientific community. Therefore, the goal of this work is to demonstrate an agreement between the damage obtained as a result of laboratory-simulated lightning and the damage achieved with the physics-based modelling in bare aluminum sheets representative of aircraft skins.

Natural lightning is a probabilistic transient high-voltage, high-current phenomenon and may occur as a result of strong electric fields present in atmosphere with the purpose to restore atmospheric equilibrium via an electrical discharge. Lightning presents a potential hazard to an aircraft in flight, and in order to simulate the effects of lightning attachment, it is conditionally characterized by the idealized voltage waveforms and current waveform components [Fisher F, Plumer J, Perala R, 2004]. Components are grouped into certain sequences to constitute lightning zones and, thus, define different levels of severity produced by lightning. A standardized lightning waveshape, designed to replicate the destructive effects of natural lightning strike in a laboratory, is schematically represented in Fig. 1. It is typically defined in terms of the four current waveforms: components A, B, C, and D. Components A and D represent high action integral current pulses, and components B and C indicate the

intermediate and continuing currents of the lightning strike, respectively. Specifically, current component C represents the long-duration currents and is expressed as a rectangular waveform of 200-800 A average current amplitude level with durations of 0.25-1 seconds to transfer 200 C (±20%) of charge. The analysis of damage inflicted by the continuing current component C is the focus of the present work. Attachment of current component C to an aircraft skin is best described in terms of interaction of the quasi-equilibrium thermal plasma discharge (an electrical arc) and a metallic cathode at atmospheric pressure in open air.

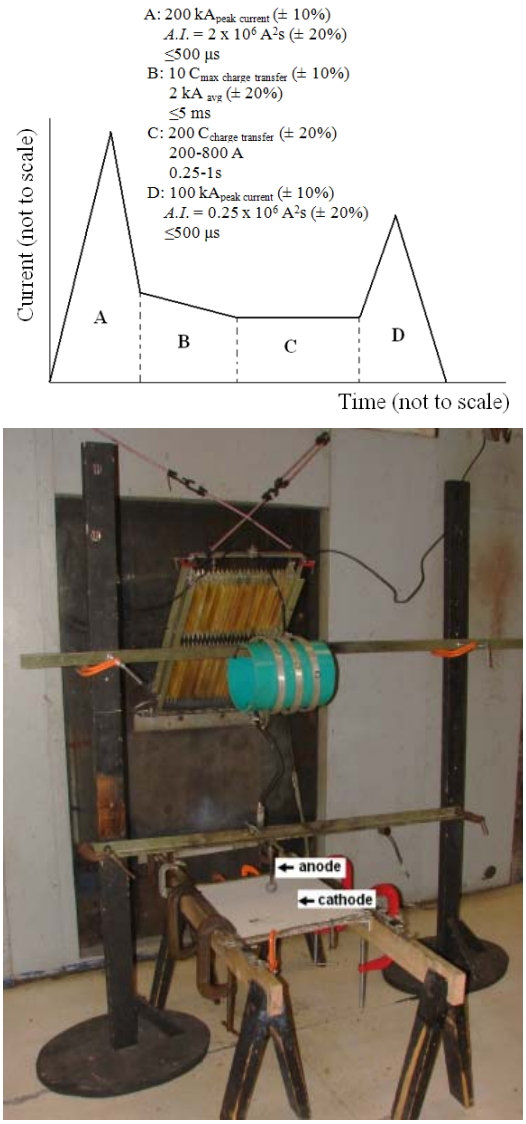

FIG. 1 HIGH-CURRENT, DIRECT EFFECTS LABORATORY LIGHTNING TESTING: SCHEMATIC OF THE STANDARDIZED SIMULATED LIGHTNING WAVEFORM WITH CURRENT COMPONENTS AND A PHOTOGRAPH OF THE TEST SETUP AT LIGHTNING TECHNOLOGIES, INC.

In low-melting point metals, like aluminum, the electric current of the arc flows through the appearing and disappearing cathode hot spots characterized by high current densities, which leads to localized intensive heating and evaporation of the cathode material from these spots [Fridman A, Kennedy L A, 2004]. As a result, in short-duration arcs, the cathode surface is damaged by the erosion process via formation of single craters on the surface [Guile A E et al., 1982], while the prolonged interaction times lead to melting of the material's bulk, and, for example, in natural lightning, formation of surface pitting, burn- or melt-through areas in metallic surfaces would be anticipated [Hagenguth J, 1949; Kostogorova-Beller Y, 2012]. The complexity of the mechanism of arc-cathode interaction often undermines the success of the physics-based modelling due to a large number of influencing factors and associated uncertainties in their quantification, thus forcing an employment of rudimentary assumptions. In addition, slight changes in experimental setup such as electrode distance, cathode surface finish, test article circuit grounding, etc. would typically result in a noticeable scatter of the damage.

For implementation of modelling, the problem lies in the precise determination of thermal flux (W/m^2) or heat rates (J/s) transferred by an electric arc to the cathode. Specifically, the subdivision of the arc potential into the cathode, anode, and the positive column regions as well as the macroscopic cathode area which contains multiple microspots of the arc attachment need to be taken into account[TestePh et al., 2004]. The power input into the cathodic layer consists of the electrical input power and a particle flux from the cathode surface [Dabringhausen L, 2002]. Following the simplified heat balance at the cathode, the heating of the cathode surface is due to the energy exchange between the positive ion current and the electrons in the cathode fall space combined with the heat of neutralization of the ions [Cobine J D, 1958]. As the cathode drop is the main source of energy for the spot, the power flux due to the ion current into the boundary layer is determined by the cathode drop voltage which is dependent on the ion current density[Rakhovskii V I, 1976]. A fraction of the heat flux is used for vaporization, while the remainder of this incoming flux is dissipated by Nottingham cooling associated with electron emission, and conduction losses into the cathode bulk, due to which formation of liquid volumes underneath the arc attachment points takes place [Coulombe S, Meunier J-L, 2000]. Complex process of the ion production and electron emission in the cathodic layer determines the cathode surface temperature. The surface temperature

is also a function of the electrode gap and the characteristics of the cathode layer such as its composition, presence of oxides and contaminants, surface roughness, and dissolved gasses [Cobine J D, 1958]. Also, the cathode surface heating strongly depends on the behavior of the arc's velocity as the cathode spot on low-boiling-point metals is in a continuous random motion which produces the multiple attachments[TestePh et al., 2004], at least prior to the achievement of sufficiently high temperatures [Fridman A, Kennedy L A, 2004]. Movement of a discharge appears in a discontinuous manner with traces consisting of a number of separate craters, implying that the discharge is fixed at a single spot only over a certain time during which the crater's dimensions grow. The highest velocities of the cathode spots correspond to the materials with low heat conductivity and melting point [Cobine J D, 1958]; transition towards the slower speeds takes place as a result of pre-heating. The slower moving spots are considered to be responsible for the highest rate of erosion [Rakhovskii V I, 1976].

The goal of the present work is to develop a computational tool based on the physics of the process and experimental evidence, able to predict damage at macroscopic scale, and discuss the influencing factors associated with the experimental setup. This work utilizes the Stefan heat conduction approach as a working hypothesis in order to model damage formation caused by melting in the aluminum alloy sheets. The numerical results are juxtaposed to the experimentally obtained damage due to the simulated lightning rectangular current waveform (component C). Based on the developed model an investigation into other metals with various thermo-physical characteristics is carried out to define a relationship between the material properties and the extent of damage.

Experiment

High-current, reverse polarity (test plate – cathode, top rod electrode – anode) direct effects lightning testing (Lightning Technologies, Inc.) was conducted on unpainted 7075-T6 aluminum alloy sheets, Fig. 1(b). Two approaches, summarized in Table 1, were utilized: 1) a time-dependent approach, during which a range of 70-770 C of charge was delivered to the test articles at constant 200A and 500A amplitude levels at discrete time steps, and 2) a fixed charge (~200 C) approach at varying amplitude levels of 50, 200, 500, and 950 A. Rectangular current waveforms (component C) were supplied to the test articles via an arc-entry by a ~1400-volt battery bank. Total circuit resistance and inductance were specifically modified for each level of amplitude. The current duration time was controlled with the 20k fuse link (West Virginia Electric) under 180 ms and with the Tenma TGP110 Pulse Generator above the 180 ms time range. Current was monitored with the T&M Research F-1000-4 current viewing resistor. Test panels were sandwiched between the metallic ground straps around the perimeter held by the metallic clamps and grounded towards the generator via a doubled array path. A fine-gage aluminum arc-initiating wire was attached to the top electrode tip and positioned in the middle of the test panel to facilitate initiation of the arc; no jet diverting electrode was used. For the time-dependent study, the separation between the electrodes was maintained at ~25 mm (1"); the anode material utilized was a ~10-mm-diameter tungsten rod (Ultra-tool). For the fixed charge transfer study, a ~10-mm-diameter zinc-plated general-purpose steel anode rod was used; the electrode separation varied within 10-50 mm to facilitate an adjustment to the necessary current amplitude, Table 1.

TABLE 1 SUMMARY OF EXPERIMENTAL TESTING

ExperimentSet	Applied Current, A	Current Duration, s	Elecrtrode Separation, mm	Sheet Thickness, mm
Fixed amplitude, varying duration, tungsten rod anode, 250 x 250 mm cathode sheets	500±13.4	0.14-1.09	25	0.51
	500±39.9	0.14-1.25	25	1.27
	200±4.7	0.35-2.45	25	0.51
	200±2.5	0.35-3.86	25	1.27
Fixed 200C charge, varying amplitude, steel rod anode, 500 x 500 mm cathode sheets	53±1.4	~3.84	10	0.51,0.71,1.27
	201±2.2	~0.99	25	0.51,0.71,1.27
	505±24	~0.39	50	0.51,0.71,1.27
	946±35	~0.2	25	0.51,0.71,1.27

Experiments were conducted at atmospheric pressure in air. Panel surfaces were thoroughly scuffed and solvent cleaned. The estimate of the damage size was based on the area encompassing the entire melt-through plus the surrounding heat affected zone due to the occasional presence of the irregular-shaped openings, rough edges, and multiple or incompletely-joined melt-through regions, Fig. 2. Formula calculating the area of an oval was used to determine the areas of 0 and 90 degrees and 45 and -45 ovals; the average of the two areas was used as the final area of the damage. The weight measurements of the 250 x 250 mm sheets aluminum plates were obtained on the Fisher Science Education compact scale with the precision of 0.1 g.

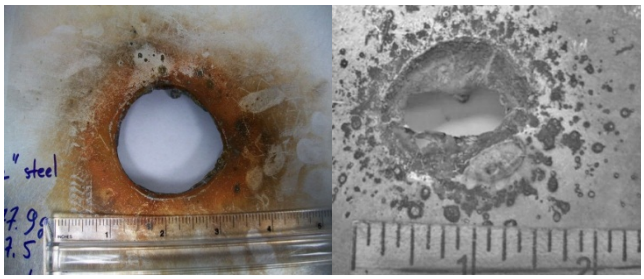

FIG. 2 LIGHTNING ARC ROOT DAMAGE ON ALUMINUM SHEETS: (a) SINGLE ORIFICE, (b) MULTIPLE ARC ATTACHMENTS AND FORMATION OF THE MELT-THROUGH EPICENTERS PRECEDING DEVELOPMENT OF A LARGER DAMAGE IN ALUMINUM SHEETS.

Model Description

The heat transfer to the cathode surface at the site of the arc attachment is described with a 2D, axisymmetric *r-t* cylindrical geometry as shown in Fig. 3(a). The heat flux brought by the arc is dissipated by heat conduction into the cathode bulk around. The cathode is heated by the arc and Joule's heating, and cooled through the convective and radiative cooling. Although the process is not axisymmetric due to the arc's irregular motion around the expanding perimeter of the damage, the jump frequency of the arc is sufficiently high allowing to assume an average radius of the growing orifice, $s(t)$, mm, which expands under the incoming heat flux, evenly distributed around the orifice's perimeter. Therefore, an assumption of the averaged process to be axisymmetric is justified. During the main stage of damage development, the arc is attached to the inner edge of the orifice while undergoing the perpetual movement around the circumference, hence, the melting front is assumed to be located at the perimeter of the orifice. On the other hand, since the thickness of the plate, h, mm, is much smaller than the radius of the experimentally observed final damage, the temperature variation across the plate's thickness was neglected. Fig. 3(b) illustrates the temperature distribution in the plate and the heat balance at the melting front.

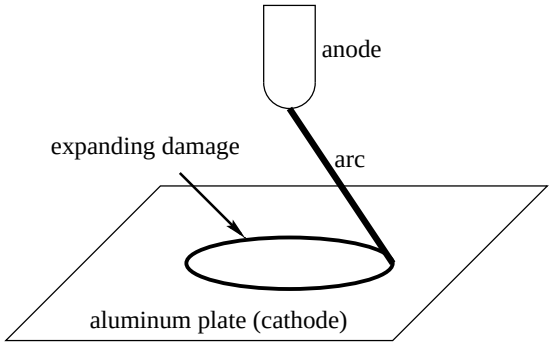

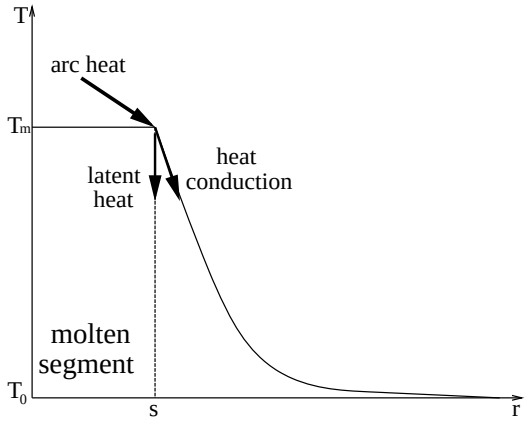

FIG. 3 SCHEMATIC OF THE MODEL: (a) GEOMETRY AND (b) TEMPERATURE DISTRIBUTION AT THE MELTING FRONT.

In the metal plate, the heat conduction is governed by

$$\rho(T)C(T)\frac{\partial T}{\partial t}=\frac{\partial}{\partial r}(k(T)\frac{\partial T}{\partial r})+\frac{k(T)}{r}\frac{\partial T}{\partial r}+j^2\rho_e-\frac{q_c(T)+q_r(T)}{h},\quad(1)$$

where ρ, g/cm^3, C, J/gK, and k, W/cmKare the density, specific heat, and thermal conductivity of the metal, respectively, Table 2. The density and specific heat are modeled as linear functions of the temperature between T_m, the melting temperature, and T_r, the room temperature at 293 K. The thermal conductivity is modeled as a piecewise quadratic function of temperature with peak value at 370K for aluminum [Powell R W, Ho C Y, Liley P E, 1966]. The current density$j$is given by $I/2\pi rh$, ρ_e is electric resistivity of the metal. The rate of convective cooling from the upper surface, q_c, is given by

$$q_c=\frac{0.54Ra^{1/4}k_a}{L}(T-T_r),\quad(2)$$

wherek_a is the thermal conductivity of air, L is the characteristic length, taken to be $s/2$, Ra is the Raleigh Number defined as

$$Ra=\frac{g\beta}{\alpha\upsilon}(T-T_r)L^3,\quad(3)$$

where g is the gravitational acceleration, β is the thermal expansion coefficient of air, α is the thermal diffusivity of air at the film temperature, $(T+T_r)/2$, and $\nu$is the kinetic viscosity of air [Incropera F, DeWitt D, 2000]. The convective cooling from the lower surface is negligible. The radiative cooling rate from the upper and lower surfaces, q_r, is given by

$$q_r=2\varepsilon\sigma(T^4-T_r^4),\quad(4)$$

whereσ is the Stefan-Boltzmann constant, e is the emissivity of the metal surface, taken to be 0.85.

The melting front is assumed to be located at the perimeter of the orifice, $T(s(t),t)=T_m$,where T_m is the melting temperature of metal. The growth rate of the damage radius is determined by the heat fluxes at the

melting front and the latent heat:

$$\frac{V_{eff} I_{arc}}{2\pi s \cdot h} = \rho L \frac{ds}{dt} - k_m \frac{\partial T}{\partial r}(s,t), \quad (5)$$

where k_m is the thermal conductivity at the melting temperature. The left-hand side represents the heat flux into the plate from the arc, with I_{arc} being the arc current and V_{eff} being the effective voltage drop in the arc-cathode region. The first term on the right-hand side corresponds to the heat flux consumed at the melting front, in which L, J/g, is the latent heat of melting; and the second term results from the heat conduction in the plate. The initial conditions of the equations are $T(r,0)=T_r$, $s(0)=0$.

In reality, the orifice's radial expansion is preceded by formation of the initial melt-through site taking place during a so-called induction time. Formation of the orifice, based on the visual observation, occurs through the formation of multiple melt-through areas, originating from the cathode spot arc attachments, which gradually grow closer to form a larger orifice, Fig. 2(b). The simplified approach of the present model neglects the induction time as it is very short in high amplitude arcs. Mathematically the damage was modeled as if it was resulting from a single, infinitesimally small arc attachment spot. Thus, the damage formation was assumed to begin at time zero at the metal melting temperature.

Results and Discussion

Comparison of Model and Experiment in Aluminum Alloy Sheets

Although macroscopically-appearing final damage intuitively implies its formation as a result of metal melting, the phenomenon of the material's transformation from solid to plasma encompasses a number of physical processes including heating, melting, heating above melting point, vaporization, ionization, chemical reactions, sputtering or ablation, partial regeneration of the molten areas, and re-solidification. The precise de-convolution and quantification of these processes individually imposes a challenge, and is largely stipulated by not only the thermo-physical characteristics of the cathode material but also its surface microstructure and the external parameters of the simulated lightning strike. Thus, the question of how much energy has been transferred by the arc to the material until the final damage has been formed needs to be addressed.

As widely discussed in the literature, two main mechanisms are proposed as a working hypothesis of the heat flux generation on the cathode surface - bombardment by the positive ions and the cathode material resistive heating [Daalder J E, 1973]. The ionic heating is typically assumed to be dominant [Fridman A, Kennedy L A, 2004], as the current densities of the order of ~10^7 A/cm^2 need to be reached by a cathode spot in order to provide appreciable contribution from the resistive heating[Charbonnier F M et al., 1964], which would cause evaporation and explosive matter release [Nemirovskii A Z, Puchkarev V F, 1992]. Material's erosion due to evaporation displays an exponential dependence of the erosion rate on current as it has been observed in Cu, Ni, and W cathodes over 100-700 A [Rakhovskii V I, 1976]. However, erosion in copper cathodes induced by up to 100A arc currents was governed by metal fusion [Guile A E, et al., 1982].

In the present work, the amount of metal loss, identified based on the plates weight measurements pre- and post- discharge, was considered negligible with respect to the calculated weight of the formed damage in each plate. The metal loss based on the ablation rates comprised only 9-11% of the rates determined based on the size of the melt-through areas, Fig. 4. In addition, a linear growth of damage can be identified. This points towards the fact that the metal melting prevailed in damage formation, while some loss of metal occurred as a result of physical splashing of the molten pool by the arc and dripping of metal off the molten edges of the formed damage. The overall computed effect of joule heating along with the convective and radiative cooling comprised less than five per cent. Therefore, damage modeling in the present work rests upon this conclusion.

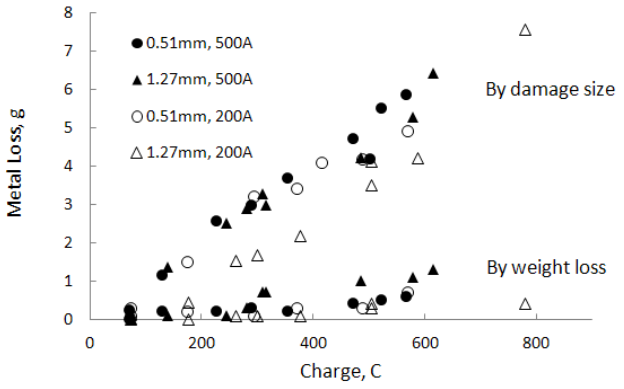

FIG. 4 METAL LOSS DUE TO MELTING INFERRED FROM THE DAMAGE SIZES AND FROM THE WEIGHT DIFFERENCE PRE- AND POST- THE DISCHARGE IN EACH PLATE.

As it was mentioned in Introduction, formation of a cathode spot results at the arc attachment in non-thermionic cathodes, which, depending on the material's nature, is characterized by a certain value of

the current density. An increase of the arc current produces multiplication of cathode spots [Rakhovskii V I, 1976]. Consideration of the cathodic spots in a state of continuous motion, common for the low-melting point metals, leads towards a concept of the effective or apparent voltage drop, V_{eff}, in proximity to the true drop through the near-cathode region, V_c, acting as the main source of energy for a single spot. Also, the uncertainties associated with quantification of processes occurring at the arc-cathode interface force the usage of the approximated cathode drop as the arc-metal interaction in the moving arcs may differ greatly from the fixed arc attachment such as in refectory cathodes. The effective voltage drop was previously utilized in modeling of duraluminium heating by the moving arcs [TestePh et al., 2004], and in investigation of the copper electrode erosion in electric arc heaters [Morotta A, Sharakhovsky L I, 1996]. Although the true cathode drop is a surface phenomenon, in the present work, the least squares fitting between the model and the experimentally obtained damage was used to infer the effective voltage of aluminum sheets in the arc attachment area, which, strictly speaking, is a summation of the true cathode drop and the voltage drop of the plate.

Based on the time-dependent data plotted inFig. 5, the effective voltage range of 10.5-11.5 V was obtained with the negligible distinction between the amplitudes and sheet thicknesses. As a comparison, the true cathode drop values for the elemental aluminum were found to be reported in the literature: 14, 15.5, 16.5, 17.2-18.6, and 18.3 V, whose measurements were obtained either via a probe located in the space charge region or as a result of extrapolation to the cathode region of the total voltage drop in short arcs [Rakhovskii V I, 1976]. The obtained effective sheet voltages appear in close proximity to the reported true cathode values.

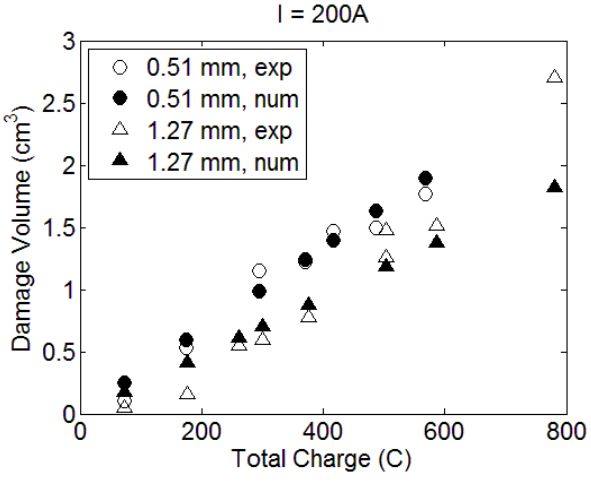

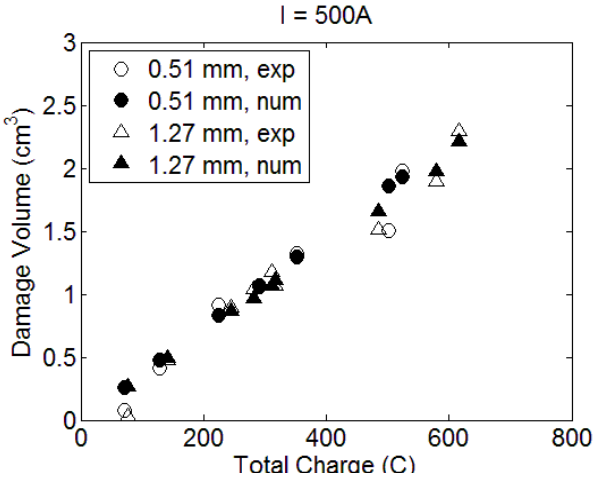

FIG. 5 COMPARISON BETWEEN THE NUMERICALLY AND EXPERIMENTALLY OBTAINED TIME-DEPENDENT DATA IN THE ALUMINUM ALLOY SHEETS. THE EFFECTIVE SHEET VOLTAGES COMPRISED 10.5 - 11.5 V; THE EXPERIMENTALLY OBTAINED RATES OF DAMAGE FORMATION COMPRISED 3.6±0.2 mm³/C.

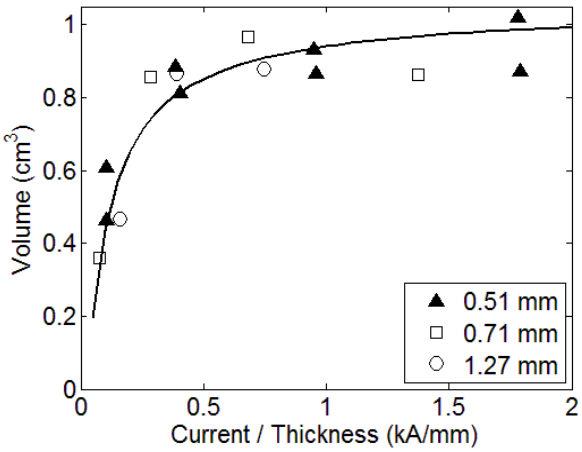

FIG. 6 PREDICTED (SOLID LINE) AND EXPERIMENTAL (POINTS) DAMAGE VOLUME IN ALUMINUM ALLOY PLATES STRICKEN BY THE ARCS OF TOTAL CHARGE 200 C AT VARIOUS AMPLITUDE, PLOTTED AS A FUNCTION OF *I*/*H* ACCORDING TO THE MODEL. THE PREDICTED CURVE WAS OBTAINED WITH V_{eff}=13 V.

Figure 6 demonstrates model prediction of the volume damage resulting from the fixed 200 C arcs at different amplitudes. With current ranging from 50 A to 950 A, the least-square fitting between computionaland experimental data indicated aneffective voltage drop of 13 V, slightly higher than the value obtained from the time-dependent data. It can be attributed tothe wider current range, the different anode material, and the varying electrode separation in the fixed charge experiments, Table 1. The true cathode voltage drop is related to the thermo-physical material properties [Nemirovskii A Z, Puchkarev V F, 1992] and its increase would be associated with an increase of the cathode heating [Rakhovskii V I, 1976]. The difference

in the obtained V_{eff} is indicative that the effective voltage drop is sensitive to the experimental parameters such as current, electrode separation, cathode material purity, surface cleanness and microstructure, in addition to the material's physical properties. The modeled results show that for a fixed charge of 200 C, the damage volume increases with the ratio of amplitude over plate thickness, *I*/*h*, towards a maximum value, at which the thermal conduction can be regarded negligible, Fig. 6. This is attributed to the relationship between arc heating rate and conductive cooling through the sheet.A higher current leads to faster heating at arc root, and less efficient conductive cooling, resulting in higher damage rate. It is also reflected in Fig. 5 for time-dependent data, where the higher damage formation rates resulted in the 500 A arcs in contrast to 200 A.

The mechanism of damage can be visualized more completely as the following: the onset of the orifice's radial expansion is preceded by an induction time, characterized by the passage of some charge without forming a complete melt-through. During this induction period, development of an association of multiple cathode spots encompassing a certain area takes place. Boiling surface of the cathode spots leads to the surface erosion with formation of the fluid micro-volumes underneath each spot, from which the heat is spread into the metal giving rise to bulk melting [Cobine J D, 1958; Coulombe S, Meunier J-L, 2000]. An appearance of multiple melt-through areas in thin sheets takes place, which gradually grow closer to form a larger orifice that subsequently keeps expanding further outwards, Fig. 2(b). A more sophisticated approach needs to be employed to realistically represent the process physics, but this is beyond the scope of this work. Based on the above arguments, it is hypothesized that the rate of damage growth is conditioned by the temperatures around the circumference, whose mean values lie within the bounds of the temperature of a single cathode spot (evaporation), as the highest limit, and the metal's near-solidus point, as the lowest limit. These surface temperatures are affected not only by the arc current but, as well, by the external experimental parameters. Experimental and theoretical determination of the relationship of damage growth rate and the cathode surface temperatures should be realized in the future, as this is one of the most fundamental relations and is important for the proper modeling of the process.

While in the proposed model the effective cathode voltage drop was identified from the macroscopic-size damage, the true origin of this quantity is complex and requires a thorough analysis of the plasma-cathode interaction. The development of a self-consistent model is thus in progress, in which the cathode drop is to be computed numerically by iterative matching of the solutions between the near-cathode plasma layer, consisting of the ionization layer and the space-charge sheath, and the cathode bulk. Generated in the ionization layer ions are accelerated by the electric field of the space-charge sheath toward the cathode surface constituting the main mechanism of the cathode heating, while the primary importance of the space-charge sheath is to impart the cathode-emitted electrons with energies sufficient to cause ionization in the ionization layer [Benilov M S, 2008]. The problem lies in the impossibility to exactly know the sheath voltage and the self-consistency of the model implies that the voltage value is to be derived from the physics governing equations for a given set of experimental conditions: the computed distribution of the cathode surface temperature based on the multidimensional heat conduction is inputted into the separately computed dependence of the current density for an assumed voltage drop, resulting from the plasma-cathode net energy flux. The total arc current is then calculated, and the procedure is repeated while adjusting the value of voltage drop to obtain the total arc current.

Damage Prediction in Other Metals under 200-500 A Arcs

It is of a practical importance for the lightning aerospace community to be able to know the extent of damage that could be formed by a lightning attachment in various structural materials. Identifying the basic relationships between lightning discharge parameters and the material properties will lead towards damage prediction. Based on the experimental evidence of the aluminum 7075 alloy sheets, the damage of a particular metal by lightning arcs can be described by a characteristic value, namely, the damage volume per unit charge, denoted by D, which is independent of current amplitude or sheet thickness. The value D=3.6±0.2 mm^3/C was obtained for the aluminum 7075 alloy from the least squares fitting of the time-dependent experimental data, Fig. 5. As a comparison, the damage rates calculated from our heat conduction model for various metals with wide-varying thermo-physical properties are presented in Table 2. For the aluminum 7075 alloy, the calculated damage rate was 3.5±0.2 mm^3/C, which agrees with the experimental value very well. Comparison of

different metals shows that damage rate decreases with increasing metal melting point, in accord with the observation of linear decrease of fusion-dominant erosion rates with increasing pure metal melting point in copper, iron, aluminum, and silver cathodes [Guile A E et al., 1982]. Such a prediction of damage by lightning for various metals could be inaccurate due to dissimilar modes of arc attachment in the refectory and cold cathodes [Lichtenberg S et al., 2002] and due to the particular cathode spot current densities achieved by different metals [Cobine J D, Gallagher C J, 1948]. Therefore, experimental validation of these values is required.

TABLE 2 PHYSICAL PROPERTIES OF SOME METALS [Haynes W M, 2012] AND CALCUATED DAMAGE RATESON 0.51-mm SHEET BY ARCS OF 200~500 A.

Metal	ϱ, g/cm³	V_c, V	T_m, C	L, J/g	C, J/gK	k,W/cmK	D_c,mm³/C
Aluminum 7075 alloy	2.79	11.0±0.5	660	397	0.897	2.37	3.5 ±0.2
Silver	10.49	14	962	105	0.235	4.29	2.5
Iron	7.87	18	1538	248	0.450	0.80	2.2
Tungsten	19.25	20	3422	192	0.132	1.73	1.0

REFERENCES

Benilov M S. "Understanding and Modeling plasma – electrode interaction in high-pressure arc discharges: a review." J Phys D: ApplPhys 41: 144001 (2008).

Charbonnier F M, Strayer R W, Swanson L W, Martin E E. "Nottingham Effect in Field and T-F Emission: Heating and Cooling Domains, and Inversion Temperature." Phys. Rev. Lett. 13: 397-401 (1964).

Cobine J D. "Gaseous Conductors: Theory and Engineering Applications." Dover Publications, New York (1958).

Cobine J D, Gallagher C J. "Current Density of the Arc Cathode Spot." Physical Review 74: 1524-30 (1948).

Coulombe S, Meunier J-L. "Theoretical prediction of non-thermionic arc cathode erosion rate including both vaporization and melting of the surface." Plasma Sources Sci. Technol. 9: 239-47 (2000).

Daalder J E. "Joule heating and diameter of the cathode spot in a vacuum arc."TH-Report 73-E-33, ISBN 90 6144 033 5 (1973).

Dabringhausen L, Nandelstadt D, Luhmann J, Mentel J. "Determination of HID electrode falls in a model lamp I: Pyrometric measurements." J. Phys. D: Appl. Phys. 35: 1621-30 (2002).

Fisher F, Plumer J, Perala R. "Lightning Protection of Aircraft." Lightning Technologies, Pittsfield, MA (2004).

Fridman A, Kennedy L A. "Plasma Physics and Engineering." Taylor & Francis, New York (2004).

Guile A E, Hitchcock A H, Dimoff K, Vijh A K. "Physical implications of an effective activation energy for arc erosion on oxidised cathodes." J. Phys. D: Appl. Phys. 15: 2341-55 (1982).

Hagenguth J. "Lightning Stroke Damage to Aircraft." Trans. AIEE 68: 1036–1046 (1949).

Haynes W M (Ed.)."CRC Handbook of Chemistry and Physics." Ed. 93, CRC Press (2012).

Incropera F, DeWitt D. "Fundamentals of Heat and Mass Transfer."Ed. 4, Wiley, New York (2000).

Kostogorova-Beller Y. "Physics of Interaction of Lightning Currents with Aluminum Sheets." J. Aircraft 49: 66-75 (2012).

Lichtenberg S, Nandelstadt D, Dabringhausen L, Redwitz M, Luhmann J, Mentel J. "Observation of different modes of cathodic arc attachment to HID electrodes in a model lamp." J. Phys. D: Appl. Phys. 35: 1648-56 (2002).

Marotta A, Sharakhovsky L I. "A theoretical and experimental investigation of copper electrode erosion in electric arc heaters: I. The thermophysical model." J. Phys. D: Appl. Phys. 29: 2395 (1996).

NemirovskiiA Z, Puchkarev V F. "Arc voltage as a function of cathode thermophysicalproperties." J. Phys. D: Appl. Phys. 25: 798-802 (1992).

Powell R W, Ho C Y, Liley P E. "Thermal Conductivity of Selected Materials." U.S. Dept. of Commerce, National Bureau of Standards (1966).

Rakhovskii V I. "Experimental Study of the Dynamics of Cathode Spots Development." IEEE Trans. Plasma Sci. 4: 81-102 (1976).

TestePh, Leblanc T, Uhlig F, Chabrerie J P. "3D modeling of the heating of a metal sheet by a moving arc: application to aircraft lightning protection." Eur. Phys. J. AP 11: 197-204 (2004).

Yulia Kostogorova-Beller graduated from University of Nebraska-Lincoln in USA with a PhD in materials engineering in August 2007.

She has served as a Research Scientist of National Institute for Aviation Research (NIAR) since October 2008. Before joining NIAR, she served as an Assistant Research Professor and Nanofiber Facility Engineer in the Department of

Engineering Mechanics, University of Nebraska-Lincoln. Her research involved manufacturing of nanofibers, their mechanical testing and structural characterization, as well as production and characterization of advanced composite materials. At NIAR she has been leading a research program entitled "Materials for Lightning Protection of Composite Airframe Structures" under the Air Force contract BAA-08-20-PKM within which she was responsible for conducting research in the area of lightning-material interaction and materials shielding effectiveness utilizing state-of-the-art lightning strike protection schemes with the purpose of identifying novel routes towards more efficient material designs.

Tianshi Lu graduated from State University of New York at Stony Brook in USA with a PhD in applied mathematics in August 2005.

He joined the department of Mathematics and Statistics in Wichita State University (WSU) in August 2008, and has been an associated professor since 2012. Before joining WSU he worked as a research associate and an assistant computational scientist at the Computational Science Center at Brookhaven National Laboratory in USA for three years. His research is on modeling and simulation of free surface and multiphase flows, and high performance computing. In particular, he has designed efficient numerical algorithms for the simulation of phase transitions, shock waves, plasmas and bubbly flows. He did the first magneto-hydrodynamic simulation of pellet ablation in a tokamak, modeled the dynamic phase transitions between compressible media, and simulated acoustic and shock waves in bubbly fluids using front-tracking technique. Dr. Lu's research on magnetohydrodynamics was funded by the Kansas NSF EPSCoR First Award.

Dr. Lu is a member of the American Physical Society, Society for Industrial and Applied Mathematics, American Society of Mathematics, and a full member of Sigma Xi, the Scientific Research Society.